A BESTEST VALIDATION STUDY OF THE DYNAMIC GROUND-COUPLED HEAT TRANSFER MODEL USED IN ACCURATE

Dong Chen[1]
[1]CSIRO Energy Transformed Flagship and CSIRO Ecosystem Sciences
PO Box 56, Highett. Vic. 3190, Australia

ABSTRACT

This paper presents the ground effective slab model used in AccuRate's simulation engine for house energy star rating in Australia. By comparing AccuRate's predictions with the results reported in the IEA BESTEST, it is demonstrated that for uninsulated slab-on-ground buildings, AccuRate's ground model performs satisfactory considering the balance between calculation speed and accuracy. Potential improvement in AccuRate's ground model has also been recommended for further development.

INTRODUCTION

Ground-coupled heat transfer (GCHT) can contribute up to around 50% of annual building heating loads (Neymark et al., 2008). Despite its significance in energy efficient building designs, rapid and reliable calculation of GCHT remains a challenge for the building simulation community. Differences in GCHT calculations around 50% or higher were reported among various simulation tools for uninsulated slab-on-ground constructions (Neymark et al., 2008).

The difficulty in GCHT calculation is mainly due to the lack of straightforward mathematical expressions for the three dimensional (3D) transient ground-coupled heat transfer. So far, the only available 3D analytical expression is the steady state GCHT solution for a rectangular slab derived by Delsante et al. (1983). This analytical expression currently provides the "mathematical truth standard" in the International Energy Agency (IEA) Building Energy Simulation Test (BESTEST) for ground-coupled heat transfer (Neymark et al., 2008). Ideally, a comparable analytical 3D transient heat transfer solution would close the GCHT problem for this simplest floor geometry. However, as mentioned in the BESTEST report, such an analytical 3D transient solution would be difficult, if not impossible, to derive (Neymark et al., 2008).

This paper describes the first time in an open literature the ground effective slab model for the simulation engine in AccuRate, which is the benchmark software for Nationwide House Energy Rating Scheme (NatHERS) used in Australia (Delsante, 2005). The model was developed by Dr Delsante based on approximate 3D expressions constructed from 2D analytical solutions. In this paper, the accuracy of the model was investigated using the relevant IEA BESTEST cases. It was demonstrated that the model gives satisfactory steady state, transient hourly and annual heat transfer, and phase shift results. The ground effective slab model provides a method for rapid dynamic GCHT calculations.

APPROXIMATE 3D EXPRESSIONS

Figure 1 schematically shows a two-dimensional (2D) slab with width B on a semi-infinite ground. By assuming the same thermal properties for the slab and the soil, and linear temperature distribution along the wall/ground interface, Delsante et al. (1983) derived an analytical solution for the transient ground-coupled heat transfer with periodic indoor and outdoor temperatures at an angular frequency Ω (1/s):

$$\begin{aligned}\tilde{Q}_{2D} = \Big\{ & \frac{2Lk(T_i - T_o)}{\pi aW}\big[\pi/4 \\ & - Ki_1(aW) + Ki_3(aW) \\ & - Ki_1(aB) + Ki_3(aB) \\ & + Ki_1(a(B+W)) - Ki_3(a(B+W))\big] \\ & + kaLBT_i\Big\}\exp(j\Omega t)\end{aligned} \quad (1)$$

where $\tilde{Q}_{2D}$ is the interior ground-coupled 2D transient heat flow (W); k the thermal conductivity (W/m·K) of the ground and L the length perpendicular to the slab width (m) and W the wall thickness (m). $a = (j\Omega/\alpha)^{1/2}$ and $j = \sqrt{-1}$, α is the ground thermal diffusivity (m^2/s) and t the time (s). Ki_1 and Ki_3 are the repeated integrals of the modified Bessel function K_0. T_i and T_o are the indoor and outdoor temperature amplitudes (°C) respectively. Both T_i and T_o may include a complex phase term $\exp(j\phi)$ to account for the phase shift relative to a specified initial start time.

Delsante et al. (1983) also obtained a steady state 2D heat transfer expression from Equation (1) by letting $\Omega \to 0$:

$$Q_{2D} = \frac{2kL(T_i - T_o)}{\pi} \times \left(\ln\left(1+\frac{B}{W}\right) + \frac{B}{W}\ln\left(1+\frac{W}{B}\right)\right) \quad (2)$$

Davies (1993) observed that Equation (2) is unsymmetrical for L and B since it is two dimensional. For a rectangular slab of $L \times B$, with the argument for symmetry between L and B, Davies (1993) constructed an approximate 3D steady state heat transfer expression by replacing L with $(L+B)$ and B with a characteristics length $LB/(L+B)$ in Equation (2). More generally, we may replace LB with the floor area A, $2(L+B)$ by the floor perimeter P, and B by a characteristic length $2A/P$. Now Equation (2) becomes

$$Q_{3D} = \frac{kP(T_i - T_o)}{\pi}\left(\ln(1+x) + x\ln(1+1/x)\right) \quad (3)$$

Here, Q_{3D} is the approximate 3D steady state heat transfer via the interior ground surface; $x = 2A/(WP)$. Results presented in Davies (1993) showed that Equation (3) gives a maximum error of 1 - 2% for a wide range of floor dimensions in comparison with the exact 3D steady state solution of Delsante et al. (1983), which is a 17-term expression. Using the same argument for symmetry between L and B, Delsante (2012) constructed an approximate 3D transient GCHT expression from Equation (1) by replacing $2L$ with perimeter P, and B by a characteristic length $2A/P$, i.e.:

$$\tilde{Q}_{3D} = \left[kGP(T_i - T_o) + kaAT_i\right]\exp(j\Omega t) \quad (4)$$

where

$$G = \frac{1}{\pi aW}\left[\pi/4 - Ki_1(aW) + Ki_3(aW) - Ki_1(2Aa/P) + Ki_3(2Aa/P) + Ki_1(a(2A/P+W)) - Ki_3(a(2A/P+W))\right] \quad (5)$$

Here, $\tilde{Q}_{3D}$ is the approximate ground-coupled 3D transient heat flow (W). It can be shown that when Ω approaches 0, Equation (4) reduces to the approximate 3D steady state heat transfer Equation (3). For the 2D case, Equation (4) reduces to the exact 2D transient solution of Equation (1).

GROUND EFFECTIVE SLAB MODEL

Delsante (1990) showed that an expression like Equation (4) can be used in building simulation tools based on a frequency response factor method. For a homogeneous 1D slab of finite thickness, the heat transfer for periodic indoor and outdoor temperatures can be described as

$$\begin{bmatrix} T_o \\ q_o \end{bmatrix} = \begin{bmatrix} S_{11} & S_{12} \\ S_{21} & S_{22} \end{bmatrix}\begin{bmatrix} T_i \\ q_i \end{bmatrix} \quad (6)$$

where q_i and q_o are the amplitudes of heat flows per unit area for interior and exterior slab surfaces respectively. From Equation (6), we have:

$$q_i = \frac{T_o - S_{11}T_i}{S_{12}} \quad (7)$$

For building simulation tools, it is desirable that the ground be represented by a 1D ground effective slab (simplified as GRES hereafter), which allows the GCHT to be calculated by Equation (6). By comparing Equation (7) with Equation (4), Delsante (1990) found that

$$S_{11} = 1 + aA/(P \times G)$$
$$S_{12} = -A/(kP \times G) \quad (8)$$

If the indoor air film resistances R_i is considered, the following equations can be used to obtain the ground-coupled heat transfer for a harmonic frequency of Ω:

$$\begin{bmatrix} T_o \\ q_o \end{bmatrix} = \begin{bmatrix} S_{11} & S_{12} \\ S_{21} & S_{22} \end{bmatrix}\begin{bmatrix} 1 & -R_i \\ 0 & 1 \end{bmatrix}\begin{bmatrix} T_i \\ q_i \end{bmatrix} \quad (9)$$

and

$$q_i = \frac{S_{11}T_i - T_o}{S_{11}R_i - S_{12}} \quad (10)$$

Equation (9) and the corresponding 3D steady state component, i.e., Equation (3), have been implemented in AccuRate's simulation engine since 1994. In the AccuRate simulation engine, the frequency response of a building is first calculated over a range of frequencies. The response to a transient pulse is then derived from the frequency responses via linear system theory (Walsh and Delsante, 1983). In the existing AccuRate engine,

frequency responses at 59 frequencies, given by $(2\pi/24)\cdot 2^{(n-39)/2}$ (n =1,2,…,59) radians per hour are evaluated. For residential buildings, an hourly simulation using AccuRate over one year period normally takes less than one minute. It is noted that the existing AccuRate engine implementation does not include the external air film resistance as S_{21} and S_{22} cannot be obtained from Equation (4) alone. An improved version of the GRES model which can account for the external air film resistance has recently been developed. The calculations of S_{21} and S_{22} and the implementation methodology in building simulation tools for this improved GRES model are detailed in Chen (2013). In the next section, the accuracy of the AccuRate GRES model is investigated using IEA BESTEST for ground coupled heat transfer (Neymark et al., 2008).

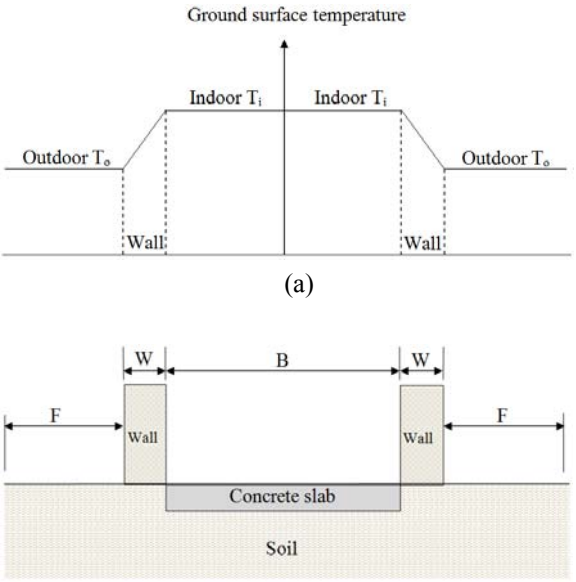

Figure 1 Schematic view of a two-dimensional slab-on-ground construction with a semi-infinite ground: (a) Temperature amplitude distributions along the ground surface; (b) Elevation view.

BESTEST VALIDATION STUDY

IEA BESTEST Cases

The IEA BESTEST for GCHT includes three "a"-series, nine "b"-series and five "c" series test cases (Neymark et al., 2008). Results from any GCHT model can be compared with "mathematical truth standard" based on the analytical solution (for Case GC10a only – see below) by Delsante et al. (1983) and "secondary mathematical truth standard" based on verified 3D numerical model results. In the IEA BESTEST report, verified numerical models for the relevant test cases include TRNSYS, FLUENT and METLAB (Neymark et al., 2008).

For the "a"-series test cases, the temperature boundary conditions are applied directly to the ground and the interior slab surfaces. The "b"-series test cases apply air film resistances to both interior slab and exterior ground surfaces, while the "c" series test cases were designed with air film resistance applied on the interior surface only. Further, "c" series test cases have relatively small far field boundary distances, i.e., small F values (refer to Figures 1 and 2 for the definition of F). In this study, all the "a"-series and "b"-series test cases, and one "c"-series test case were used for validating AccuRate GRES model. Table 1 briefs the descriptions and main parameters for the 13 test cases. For all the steady state test cases, the interior and exterior temperatures are maintained at 30°C and 10°C respectively. The hourly GCHT for the steady state cases was obtained with AccuRate simulation at the end of 11th year when it approaches steady state. For test cases with harmonic variation in the exterior temperature, the interior temperature is maintained at 30°C while the exterior temperature is described by the following equation (Neymark et al., 2008):

$$T_o = 10 - 6\cos\left(\frac{2\pi(IDay-15)}{365}\right) - 2\cos\left(\frac{2\pi(IHour-4)}{24}\right) \quad (11)$$

Here *IDay* is the day counter from 1 to 365; *IHour* is the daily hour counter from 1 to 24 with reset to 1 after end of a day. The hourly GCHT for a year were obtained from the output of AccuRate simulation at the 11th year after it approaches periodic steady state.

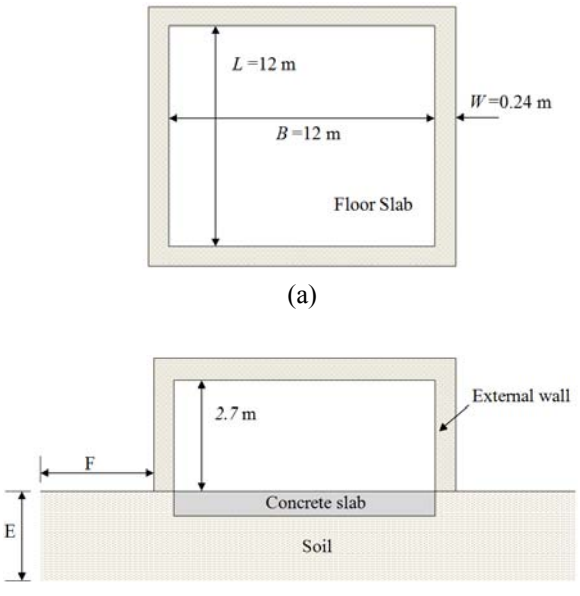

Figure 2 Schematic view of a three-dimensional slab-on-ground used in IEA BESTEST (Neymark et al., 2008): (a) Plan View; (b) Elevation view (E is the deep ground depth and F is the far field boundary)

Case GC10a is a 3D steady state test case for a rectangular slab on a semi-infinite ground configuration with linear temperature distribution along the wall/ground interface. The GCHT result for Case GC10a can be compared against the 3D analytical solution by Delsante et al. (1983). Case GC30a is also a steady state test case with the same slab-on-ground configuration as Case GC10a, except that: i) the wall/ground interface is adiabatic; ii) 30 m deep ground has a uniform temperature at 10°C which is the annual average ambient temperature; iii) far field ground 20 m away from the external wall surface has an adiabatic boundary condition. The rectangular slab geometry for Case GC30a is schematically shown in Figure 2. Case GC40a is exactly the same as Case GC30a except that the exterior ground surface temperature is periodic as defined by Equation (11). For all the cases listed in Table 1, the ground was assumed to have a uniform thermal conductivity of 1.9 W/m·K, density of 1490 kg/m^3 and specific heat at 1800 J/m^3 except Case GC80b which has a thermal conductivity of 0.5 W/m·K. Detailed descriptions of the test cases can be found in the IEA BESTEST document (Neymark et al., 2008).

Comparisons of GCHT Results

Table 2 compares the predicted ground-coupled steady state heat transfer and steady periodic annual heat transfer results from the AccuRate GRES model and those reported in the IEA BESTEST from analytical solution by Delsante et al. (1983) and verified 3D numerical models (Neymark et al., 2008). It was found that AccuRate GRES model gives predicted floor heat transfer within 11% from the analytical solution and the averages of verified numerical model results except test cases GC50b and GC55b.

For all the test cases listed in Table 1 except test Case GC10a, uniform temperature of 10 °C is applied at the deep ground boundary. Due to the relatively shallow deep ground depth for Case GC50b (large floor area) and Case GC55b (shallow deep ground depth), there are substantial core heat transfer directly into the deep ground from these two cases. The analytical solution presented in this study assumes a semi-infinite ground and thus cannot be used for GCHT calculation for Cases GC50b and GC55b. Therefore, Case GC50b and Case GC55b were excluded in the remaining validation study in this paper. It should also be noted that all the cases in Table 1 except Case GC10a assume adiabatic boundary condition at the wall/ground interface. Hagentoft (1996) showed that for normal building dimensions, the approximation of adiabatic walls gives a 5-10% higher heat loss than given by a linear temperature drop under the walls. Consequently, these two differences in the model assumptions explain that in general, the estimated heat transfer from the AccuRate GRES model were slightly lower than the averages of the verified numerical model results for cases with no or very small air film resistances, i.e., Cases GC30a, GC30b, GC40a, GC40b, GC45b and GC80b.

When there are realistic air film resistances applied on the ground surfaces, i.e., Cases GC40c, GC60b, GC65b and GC70b, the GRES model slightly over-predicts the ground-coupled heat transfer. The reason is that the GRES model does not account for the varying heat transfer rate and implicitly assumes uniform heat transfer rate along the ground surface by using Equation (6) or (9). This is not an issue when the ground surface temperatures are known and are directly used in calculating the ground-coupled heat transfer since Equation (6) together with Equation (8) are exact representations of Equation (4). Equation (3) is also the direct representation for the steady state heat transfer calculation. However, this treatment can reduce the calculation accuracy when there are realistic air film resistances above the ground surfaces. Due to the short path, the ground-coupled heat transfer rate near the wall edges is relatively high or the local thermal resistance of the ground is relatively small. The air film resistance reduces heat transfer more effectively at locations near the wall edges than those away from the walls. The net impact of ignoring the local heat transfer non-uniformity is an overestimation of the total GCHT.

This is also demonstrated by the peak-hour heat transfer results in Table 3 for Case GC70b which has realistic air film resistances on both the interior and exterior ground surfaces. The GRES model over-predicts 12.2% in the peak–hour heat transfer in comparison with the verified numerical models. It should be noted that the AccuRate GRES model does not account for the external air film resistance, which can also contributes to the GCHT over-prediction for Case 70b. With the same reason, the GRES model over-predicts slightly for Case GC40c. For all the other test cases, the maximum difference in peak-hour heat transfer between the GRES model and the verified numerical models is -8.2% which is mainly caused by the differences in the steady state components due to boundary condition differences.

Table 4 compares the phase shift results from the AccuRate GRES model and the verified numerical models for harmonic temperature variation test cases. The phase shift is defined as the difference between the hour with the coldest ambient temperature and the hour with the highest heating load. It was found that the GRES model gives satisfactory phase shift predictions which are within 7 days of those

predicted by the average of the verified numerical models. Figures 3 and 4 compare the hourly heat transfer results for test Cases GC40a and GC40c respectively. The hourly ground-coupled heat transfer results predicted by the GRES model are in satisfactory agreement with those by the verified numerical models and lie between the results by various building simulation tools.

It was demonstrated that despite the deficiencies in the GRES model in terms of not considering external air film resistance and the implicit assumption of uniform heat transfer rate, the good agreement for the IEA BESTEST cases suggests that the AccuRate GRES model can provide fast and satisfactory GCHT calculations for uninsulated slab-on-ground constructions. Further improvement in the AccuRate GRES model is possible by addressing these two deficiencies. An improved GRES model which takes into account the external air film resistance has been reported in another submission (Chen, 2013).

CONCLUSION

This paper presents AccuRate's ground effective slab model for GCHT calculations for uninsulated slab-on-ground constructions. By comparing predictions from the AccuRate GRES model with the results reported in the IEA BESTEST, it was demonstrated that for uninsulated slab-on-ground buildings, the AccuRate GRES model performs satisfactory in the GCHT calculations considering the balance between calculation speed and accuracy. Potential improvement in AccuRate's ground model was also discussed for future development. Dynamic calculation for insulated slab-on-ground is more challenge and future research is required on analytical solutions for insulated slab-on-ground.

NOMENCLATURE

a = $\left(j\Omega/\alpha\right)^{1/2}$
A = floor area
B = floor width
E = deep ground boundary distance
F = far field boundary distance
h = ground surface heat transfer coefficient
$IDay$ = day counter from 1 to 365
$IHour$ = daily hour counter from 1 to 24
k = thermal conductivity of the ground
L = building length
P = floor perimeter
Q = steady-state heat flow
$\tilde{Q}$ = transient heat flow
q_i = indoor amplitude of heat flux
q_o = outdoor amplitude of heat flux
t = time
T_i = indoor temperature amplitude
T_o = outdoor temperature amplitude
W = wall thickness
x = $2A/(WP)$

Symbols
Ω = angular frequency
α = ground thermal diffusivity

Subscripts
i = interior
o = exterior

ACKNOWLEDGEMENT

The study was co-funded by Australian State and Territory government, and the Department of Climate Change and Energy Efficiency, Australian Federal Government. The author would like to thank Dr Angelo Delsante's generous support and advice during this study.

REFERENCES

Delsante, A.E., Is the new generation of building energy rating software up to the task? - A review of AccuRate. ABCB Conference 'Building Australia's Future 2005', Surfers Paradise, Australia, 11-15 September 2005.

Chen, D. Dynamic Three-Dimensional Heat Transfer Calculation for Uninsulated Slab-on-ground Constructions, Energy and Buildings, in printing, 2013.

Davies, M.G. Heat loss from a solid ground floor. Building and Environment 28 (1993):347-359.

Delsante, A.E., Stokes, A.N., Walsh, P.J. Application of Fourier Transforms to Periodic Heat Flow into the Ground under a Building, International Journal of Heat Mass Transfer 26(1) (1983) 121-132.

Delsante, A.E. A comparison between measured and calculated heat losses through a slab-on-ground floor, Building and Environment 25 (1990) 25-31.

Delsante, A.E. private communication, 2012.

Hagentoft, C.E. Heat losses and temperature in the ground under a building with and without ground water flow-I. Infinite ground water flow rate. Building and Environment 31(1) (1996): 3-11.

Neymark, J., Judkoff, R., Beausoleil-Morrison, I., BenNakhi, A., Crowley, M., Deru, M., Henninger, R., Ribberink, H., Thornton, J., Wijsman, A., Witte, M. International Energy Agency Building Energy Simulation Test and Diagnostic Method (IEA BESTEST) In-Depth Diagnostic Cases for Ground Coupled Heat Transfer Related to Slab-on-Grade Construction, NREL/TP-550-43388. Golden, Colorado, USA: National Renewable Energy Laboratory, 2008.

Walsh, P.J., Delsante, A.E. Calculation of the thermal behaviour of multi-zone buildings, Energy and Buildings 5 (1983) 231-242.

Table 1 Input parameters for ground coupling in-depth diagnostic test cases, adapted from (Neymark et al., 2008)

Case	Description	Dynamic	Slab Dimen. (m × m)	h_i** (W/m²K)	h_o** (W/m²K)	Ground Depth (m)	Far-Field Boundary (m)	Cond. (W/mK)	Comments
GC10a	Analytical Base Case	steady	12 × 12	Direct temp*	Direct temp	infinite	infinite	1.9	Liner temperature for wall/ground interface
GC30a	Comparative Base Case for "a"-series	steady	12 × 12	Direct temp	Direct temp	30	20	1.9	Adiabatic wall/ground interface
GC30b	Comparative Base Case for "b"-series	steady	12 × 12	100	100	15	15	1.9	
GC40a	Harmonic variation	harmonic	12 × 12	Direct temp	Direct temp	30	20	1.9	
GC40b	Harmonic variation	harmonic	12 × 12	100	100	15	15	1.9	
GC40c	Harmonic variation	harmonic	12 × 12	7.95	Direct temp	15	8	1.9	Realistic interior film resistance
GC45b	Aspect Ratio	harmonic	36 × 4	100	100	15	15	1.9	
GC50b	Large Slab	harmonic	80 × 80	100	100	15	15	1.9	High core heat transfer fraction
GC55b	Shallow Deep Ground Temp	harmonic	12 × 12	100	100	2	15	1.9	Shallow deep ground. High core heat transfer
GC60b	h_i	steady	12 × 12	7.95	100	15	15	1.9	Realistic interior film resistance
GC65b	h_i and h_o	steady	12 × 12	7.95	11.95	15	15	1.9	Realistic film resistances
GC70b	Harmonic, h_i and h_o	harmonic	12 × 12	7.95	11.95	15	15	1.9	Realistic film resistances
GC80b	Ground Conductivity	harmonic	12 × 12	100	100	15	15	0.5	

* temperature applied directly to the ground surface; ** h_i and h_o are the interior and the exterior ground surface heat transfer coefficients.

Table 2 Comparison of floor heat transfer from the GRES model, CSIRO analytical solution and verified numerical models (Neymark et al., 2008)

Floor Heat Transfer	**Analytical Solution**	**Verified Numerical Models**			**AccuRate GRES CSIRO**	**Diff. Between GRES and Q.A. Mean (%)**
	CSIRO (Delsante et al., 1983)	**TRNSYS TESS**	**FLUENT PAAET**	**MATLAB DIT**		
GC10a, Steady State (W)	2433	2427	2425	2432	2403	-1.0%
GC30a, Steady State (W)		2642	2585	2695	2403	-9.0%
GC30b, Steady State (W)		2533	2504	2570	2367	-6.6%
GC40a, Steady Periodic (kWh/annual)		23033	22761	23609	21064	-9.0%
GC40b, Steady Periodic (kWh/annual)		22099	21932	22513	20754	-6.4%
GC40c, Steady Periodic (kWh/annual)		18649	18598	18873	18892	1.0%
GC45b, Steady Periodic (kWh/annual)		32758	32456	33483	30661	-6.8%
GC50b, Steady Periodic (kWh/annual)		277923	277988	281418	200572	-28.1%
GC55b, Steady Periodic (kWh/annual)		35075	34879	35491	20754	-41.0%
GC60b, Steady State (W)		2113	2104	2128	2156	2.0%
GC65b, Steady State (W)		1994	1991	2004	2156	8.0%
GC70b, Steady Periodic (kWh/annual)		17396	17434	17552	18892	1.0%
GC80b, Steady Periodic (kWh/annual)		6029	5939	6151	5387.2	-10.8%

* "Q.A. Mean" is the average of verified numerical model results.

Table 3 Comparison of annual peak-hour floor heat transfer results between the GRES model and verified numerical models (Neymark et al., 2008)

Annual Peak-hour Floor Heat Transfer (W)	**Verified Numerical Models**			**AccuRate GRES CSIRO**	**Diff. Between GRES and Q.A. Mean (%)**
	TRNSYS TESS	**FLUENT PAAET**	**MATLAB DIT**		
GC40a	3087	3042	3174	2846	-8.2%
GC40b	2941	2914	3002	2834	-4.0%
GC40c	2454	2444	2487	2539	3.2%
GC45b	4444	4396	4551	4230	-5.2%
GC70b	2254	2259	2276	2539	12.2%
GC80b	776	763	794	750.3	-3.5%

Table 4 Comparison of the phase shift (hours) for floor peak heat transfer results between the GRES model and verified numerical models (Neymark et al., 2008)

Phase Shift for Floor Conduction Peak (hours)	**Verified Numerical Models**			**AccuRate GRES CSIRO**	**Diff. Between GRES and Q.A. Mean (hours)**
	TRNSYS TESS	**FLUENT PAAET**	**MATLAB DIT**		
GC40a (kWh/annual)	416	416	416	432	16
GC40b (kWh/annual)	417	465	441	419	-22
GC40c (kWh/annual)	562	562	538	501	-52
GC45b (kWh/annual)	417	441	441	396	-37
GC70b (kWh/annual)	660	659	660	501	-159
GC80b (kWh/annual)	568	591	567	418	-157

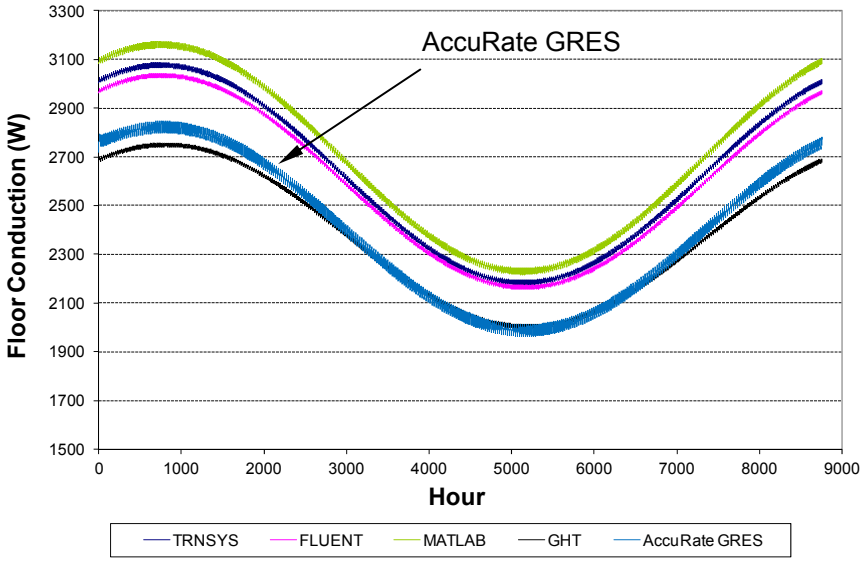

Figure 3. Comparison of predicted ground-coupled heat transfer for test Case GC40a

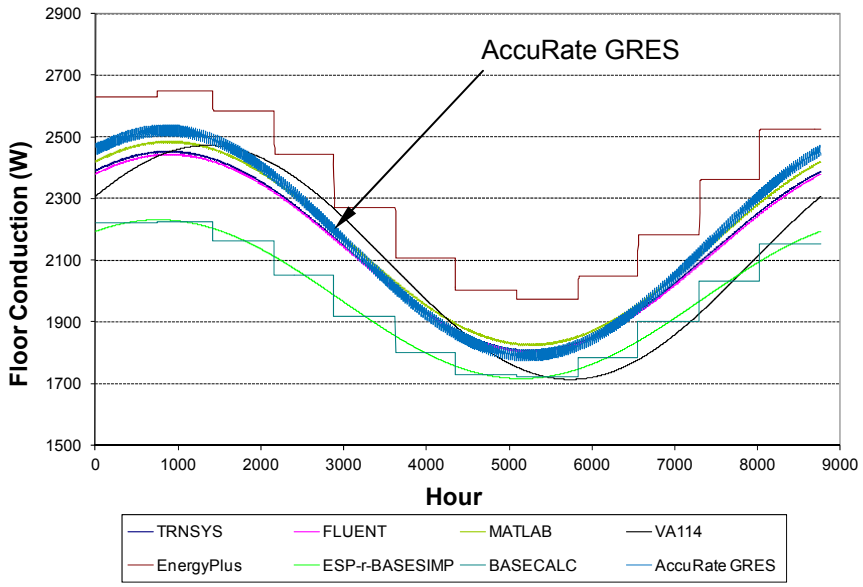

Figure 4. Comparison of predicted ground-coupled heat transfer for test Case GC40c